CHIN. PHYS. LETT. Vol. 36, No. 9 (2019) 098501

An Improved Room-Temperature Silicon Terahertz Photodetector on Sapphire Substrates *

Xue-Hui Lu(鲁学会)[1,2**], Cheng-Bin Jing(敬承斌)[1**], Lian-Wei Wang(王连卫)[1], Jun-Hao Chu(褚君浩)[1,3]

[1]*Key Laboratory of Polar Materials and Devices (Ministry of Education), Institute of Functional Materials, Department of Materials, School of Physics and Electronic Science, East China Normal University, Shanghai 200241*

[2]*Shanghai Institute of Intelligent Electronics & Systems, Fudan University, Shanghai 200433*

[3]*State Key Laboratory of Infrared Physics, Shanghai Institute of Technical Physics, Chinese Academy of Sciences, Shanghai 200083*

(Received 25 June 2019)

We design and fabricate a good performance silicon photoconductive terahertz detector on sapphire substrates at room temperature. The best voltage responsivity of the detector is 6679 V/W at frequency 300 GHz as well as low voltage noise of 3.8 nV/Hz$^{1/2}$ for noise equivalent power 0.57 pW/Hz$^{1/2}$. The measured response time of the device is about 9 μs, demonstrating that the detector has a speed of >110 kHz. The achieved good performance, together with large detector size (acceptance area is 3 μm×160 μm), simple structure, easy manufacturing method, compatibility with mature silicon technology, and suitability for large-scale fabrication of imaging arrays provide a promising approach to the development of sensitive terahertz room-temperature detectors.

PACS: 85.60.Gz, 73.40.Sx, 95.55.Rg DOI: 10.1088/0256-307X/36/9/098501

In recent years, the extensive application of terahertz (THz) technology in many scientific and technological fields[1–3] has aroused widespread concern and research.[4–6] THz technology has been widely used in a variety of potential applications, such as the chemical composition analysis,[7,8] integrated circuit failure analysis,[9] homeland security,[10] detection of skin,[11,12] cancer diagnosis,[13] and DNA chips.[14] To ensure a high performance of the applications in these areas, it is highly desired to develop efficient THz components such as THz detectors,[1,2,10,15] emitters,[16,17] phase shifters[18] and modulators.[19] However, due to the lack of high power THz sources, the THz wave band ranging from 300 GHz to 10 THz has been referred to as the 'terahertz gap'.[20] In particular, the development of an excellent THz detector is considered to be an important challenge in the field of THz technology. Commercially available THz detectors are based on thermal sensing elements that are very slow (10–400 Hz modulation frequency for Golay cells or pyroelectric elements, while capable of reaching noise equivalent powers (NEPs) in the 10^{-10} W/Hz$^{1/2}$ range). Other uncooled THz detectors are based on Schottky barrier diodes (SBDs)[21–24] and field-effect-transistors (FETs)[10,25,26] which operate best below 500 GHz due to their capacitance or transient time response. Nevertheless, the mechanism of FET THz detection is a weakly second-order nonlinear response to THz waves. The low quantum efficiency of the detectors limits the performance for detection. Furthermore, Schottky diodes and CMOS/SiGe transistor detectors cannot be impedance matched to a planar antenna over a wide frequency due to the device capacitance.

In the hope of improving the disadvantages of present THz detectors, electromagnetic induced well (EIW) theory was proposed to provide a new photoelectric effect mechanism for extremely sensitive THz detection, which utilizes the wave of THz radiation to emit electrons from metals into a semiconductor in the wrapped metal-semiconductor-metal (MSM) structure with a subwavelength gap.[27] The physical mechanism of the EIW theory shows that as external THz radiation with photon energy far below the semiconductor bandgap impinges onto the MSM structure, potential wells would be induced to trap carriers originating from the metal contacts because of the great difference in the electron concentration between the metal and the semiconductor. Considering the intrinsic relation of electric potential and electric field, electrons in the metals are dislodged into the well due to its low potential energy. Then, electrons from the metals are emitted and trapped in the well located at the semiconductor, thus changing the conductivity of the semiconductor element. By collecting the photovoltage between the two metal contacts during the process, the impinged THz radiation could be detected.

Based on the EIW theory, the fabricated detectors utilizing mercury cadmium telluride (MCT) as the semiconductor element of the designed MSM structure indicate good performance at room temperature, with NEPs of 3.5 fW/Hz$^{1/2}$ at 300 GHz and 8.9 fW/Hz$^{1/2}$ at 650 GHz.[28] To further develop the application of the EIW theory and demonstrate its generality, we fabricated a room-temperature silicon photoconductive terahertz detector on silicon-on-insulator(SOI) substrates previously. From the measured experimental data, the detector's NEP reaches 1 pW/Hz$^{1/2}$ at 309 GHz and 3 pW/Hz$^{1/2}$ at 648 GHz. Due to the

*Supported by the National Natural Science Foundation of China under Grant Nos 61775060 and 61275100.

**Corresponding author. Email: xhlu@ee.ecnu.edu.cn; cbjing@ee.ecnu.edu.cn

© 2019 Chinese Physical Society and IOP Publishing Ltd

field-enhanced emission of carriers through traps near the buried-oxide/silicon interface, high junction leakage current would occur on SOI substrates.[29–31] The leakage current would greatly decrease the responsivity of the detector, which could reduce the device performance. In contrast with SOI where the thin (on the order of μm) silica cladding layer is prone to leakage to the silicon substrate, the sapphire substrate could eliminate any potential substrate leakage.[32] Hence, we propose a kind of room-temperature MSM structure Si photoconductive terahertz detectors on sapphire substrates, which have a speed of >110 kHz and the minimum NEP of 0.57 pW/Hz$^{1/2}$ at 300 GHz. The typical size of the Si detectors are 3 μm in width and 160 μm in length, which are much larger than those of the commonly used SBDs and FETs. The larger feature size has resulted in better compatibility with common optical systems, as well as good scalability in combining THz detection and mainstream silicon technology, and large arrays have been integrated by mature technology in micrometer class, in avoiding of the complicated nanoscale techniques.

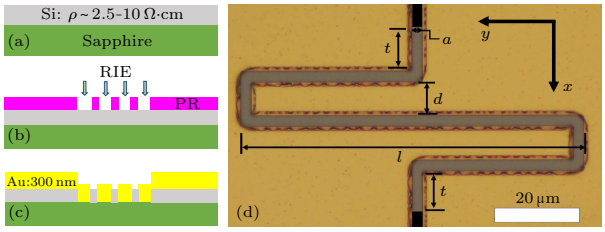

Fig. 1. (a) SOS substrate of the device. The top layer Si (n-type) is 300 nm in thickness with a resistivity of 2.5–10 Ω·cm. (b) Etching top layer Si bridge by RIE. (c) Sputtering Au onto the substrate as a pad with thickness of 300 nm, (d) Optical photo of the detector (spacing length of the detector $a = 3$ μm, transverse length of the detector $l = 80$ μm, interval length of the detector $d = 10$ μm and $t = 10$ μm).

To increase the effective acceptance area of the device, a cross-finger structure is designed and the device channel's length l is set to be 80 μm (as shown in Fig. 1(d)). The response of the device increases with the decrease of spacing length a and the thickness of the semiconductor, thus the photoactive element was optimized to be with thickness of 300 nm and the spacing length a of 3 μm. The fabrication process of the detectors is briefly described as follows. First, the top layer Si as a thin film on the SOS substrate was rinsed in acetone and ethyl alcohol. The photoactive elements were then etched out by photolithography and the excess silicon is removed by reactive ion etching (RIE) methods, followed by a second photolithography performed to protect the photoactive element while forming the electrode patterns on the SOS substrate. Second, Au electrodes of 300 nm thickness on top of a 30-nm-thick titanium intermediate layer were sputtered onto the substrate by magnetron sputtering. Finally, the samples were rinsed again in acetone and ethyl alcohol before being separated as single detector units, and a Au lead-in wire was spot-welded onto the end of each Au electrode. Both the top and the two side walls of the silicon are covered with Au, which prevents the leakage of THz radiation from the two sides and achieves a large optical gain. As can be seen from Fig. 1(d), the measured length of the photoactive region is approximately close to the designed value.

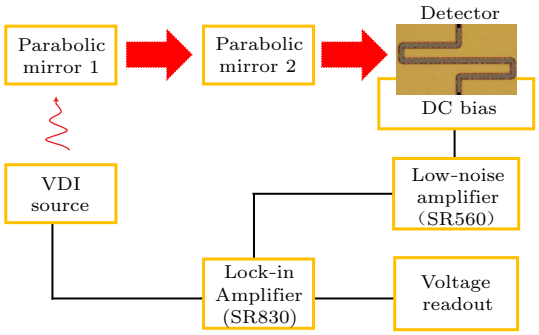

Fig. 2. Schematic diagram of the measurement system.

To demonstrate the performance of the detector, we measured the response of the detector irradiated by a THz source in the range 266–358 GHz at power intensity of 0.5 mW/cm^2 and in the range 624–712 GHz at 0.4 mW/cm^2. The I–V characteristics of our device is measured sing a Keithley 4200 parameter analyzer with the bias current swept from −5 mA to 5 mA, and the resistance is determined to be 25 Ω for the device studied. After that, to calibrate the broadband nature of the designed device, it is wirebonded and illuminated by a linearly polarized microwave source (Agilent E8257D) with a frequency tunable from 20 to 40 GHz, a VDI multiple frequency multiplier with a frequency tunable from 266 GHz to 358 GHz or from 624 GHz to 712 GHz.

Figure 2 shows the schematic diagram of the measurement system. To improve the signal-to-noise ratio, the radiation is focused to yield the largest possible signal to the detector by two off-axis parabolic mirrors, which increase the energy density impinging onto the detector. During the whole measurement, a bias current of 5 mA was applied onto the detector. The received power at every THz frequency is calibrated with a power meter (Ophir, 3A-P-THz) and the photovoltage spectra are normalized to calculate the responsivity. The THz radiation is modulated by a square waveform at the frequency of 1 kHz. The optoelectric responsivity is recorded using a low noise amplifier (SR560) connected to a lock-in amplifier (SR830). It is demonstrated that the terahertz radiation is focused at the center of the detector. All the experiments are performed in ambient environment at room temperature, and it is observed that the photovoltage is linear with incident power and linearity is independent of the irradiation intensity, corroborating again the power dependence of the optoelectric effect.

The incident power of the detector is proportional to the active area of the device. For TM wave in the x

direction of the MSM structure, $S_{0x} = 3\,\mu\text{m}\times160\,\mu\text{m}$ and for TM wave in the y direction of the MSM structure, $S_{0y} = 3\,\mu\text{m}\times40\,\mu\text{m}$. The measured output voltage in the x direction is four times that in the y direction, which is proportional to the active area of the device. Thus the voltage responsivity of the device in the y direction is almost the same as that in the x direction. First, we measured the response of the detector in 266–358 GHz and 624–712 GHz along the x direction. Second, the detector element was replaced by a power meter (Ophir, 3A-P-THz) to record the total incident power under the exact same measurement conditions. Finally, The responsivity of the detector R_v was calculated using $R_\text{v} = \frac{R_0\times\pi D_0^2}{4P_0\times S_0}$, where R_0 is the detector's responsivity to the source signal, D_0 is the spot diameter of the impinging THz radiation, P_0 is the recorded total incident power of the source signal, and S_0 is the area of the photoactive element of the detector. As shown in Figs. 3(a) and 3(b), the responsivity is mostly greater than 1000 V/W in the 266–358 GHz waveband and over 500 V/W in the 624–712 GHz waveband, respectively. Consistent with the VDI source, the best responsivities of 6679 V/W and 2333 V/W appear at 300 GHz and 645 GHz, respectively. We also measured the noise level of the detector, which allowed us to further estimate the NEP of the detector. The voltage noise spectrum is acquired on a spectrum analyzer with a low-noise preamplifier at a voltage gain of 1000. To minimize the external interference, the measurement is carried out in a shielded room. Figure 3(c) shows that the measured voltage noise of the device biased at 5 mA is $S_\text{v} = 3.8\,\text{nV/Hz}^{1/2}$. In terms of NEP=$S_\text{v}/R_\text{v}$, the NEP of the detector for the same signal mostly remains smaller than $10\,\text{pW/Hz}^{1/2}$, while the minimum NEPs are $0.57\,\text{pW/Hz}^{1/2}$ and $1.6\,\text{pW/Hz}^{1/2}$ at 300 GHz and 645 GHz, respectively. We can say that the detector has excellent characteristics.

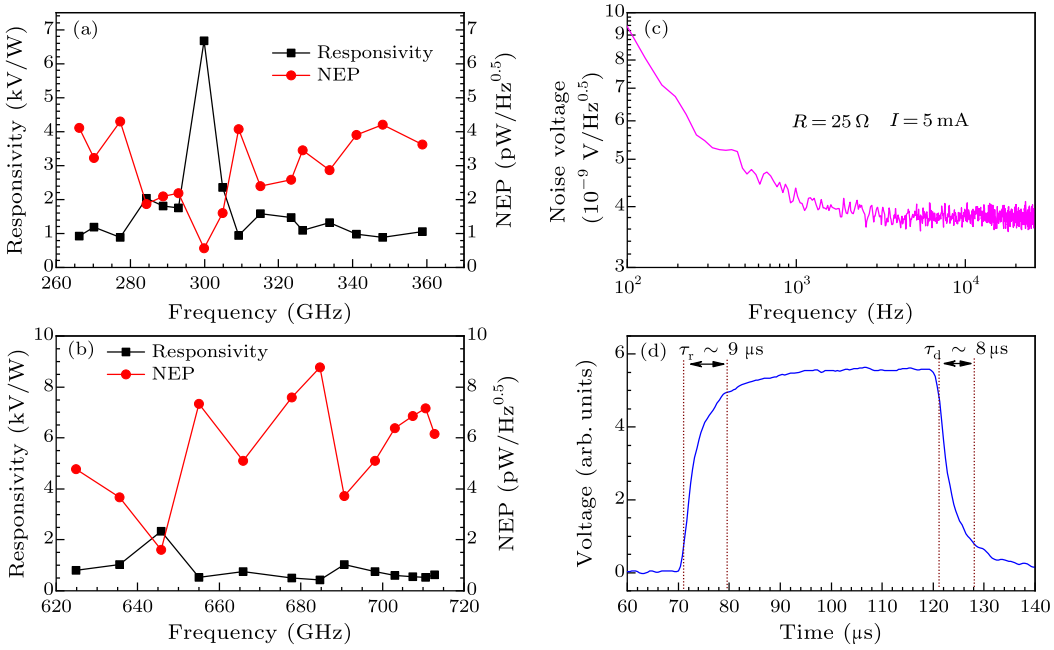

Fig. 3. (a) Responsivity and NEP of the device in the range from 266 GHz to 358 GHz, the bias current is $I = 5$ mA, the largest responsivity is 6679 V/W and the best NEP is about $0.57\,\text{pW/Hz}^{1/2}$ at around 300 GHz. (b) Responsivity and NEP of the device from 624 GHz to 712 GHz and the bias current is $I = 5$ mA, the best NEP is about $1.6\,\text{pW/Hz}^{1/2}$ at around 645 GHz. (c) Noise spectra of the detector for $R = 25\,\Omega$ and $I = 5$ mA, the noise voltage is about $3.8\,\text{nV/Hz}^{1/2}$ at the modulation frequency over 1000 Hz. (d) Response time measurement with the rise time $\tau_\text{r} \sim 9\,\mu\text{s}$ and fall time $\tau_\text{d} \sim 8\,\mu\text{s}$.

The time constant is a key parameter that indicates the response speed of the detector. Thus, a photodetector with a small response time is usually desired to allow for certain applications, such as fast-rate imaging. The response time of the photodetector is determined by measuring the time between 10% and 90% of the generated signal under the modulated excitation.[33] We use signals at 40 GHz with a modulation frequency of 20 kHz generated by a signal generator (Agilent E8257D). As shown in Fig. 3(d), the rise time τ_r (from 10% to 90% of the maximum) is 9 μs, whereas the fall time τ_d (from 90% to 10% of the maximum) is 8 μs, demonstrating the superior performance of our designed device.

In conclusion, we have designed and fabricated a THz photodetector with an MSM structure using the n-type silicon fabricated on sapphire wafer to demonstrate the novel EIW photoconductivity theory. The responsivity is 6679 V/W referenced to the incident power and a minimum NEP is $0.57\,\text{pW/Hz}^{1/2}$ at 300 GHz, including the effects of extrinsic losses and noises generated by the integrated amplifier cir-

cuit. Compared with Si devices on SOI substrates, the voltage responsivity of Si devices on sapphire substrates increases by nearly 98%, while the NEP decreases by nearly 43% at 300 GHz, reflecting that our devices have more excellent performance. The measured response time 9 μs shows that the detector has a good response speed. Furthermore, the good uniformity and the fabrication process based on the standard silicon process is quite simple. It can be predicted that this detector will be a suitable component of THz focal-plane arrays for fast imaging and communication, as well as for detection of materials.

References

[1] Tonouchi M 2007 *Nat. Photon.* **1** 97
[2] Ferguson B and Zhang X C 2002 *Nat. Mater.* **1** 26
[3] Fan R H, Zhou Y, Ren X P et al 2015 *Adv. Mater.* **27** 1201
[4] Ulbricht R, Hendry E, Shan J et al 2011 *Rev. Mod. Phys.* **83** 543
[5] Wu Y, La-o-vorakiat C, Qiu X et al 2015 *Adv. Mater.* **27** 1874
[6] Hanham S M, Fernández-Domínguez A I, Teng J H et al 2012 *Adv. Mater.* **24** OP226
[7] Ho L, Pepper M and Taday P 2008 *Nat. Photon.* **2** 541
[8] Davies A G, Burnett A D, Fan W et al 2008 *Mater. Today* **11** 18
[9] Yamashita M, Kawase K, Otani C et al 2005 *Opt. Express* **13** 115
[10] Vicarelli L, Vitiello M S, Coquillat D et al 2012 *Nat. Mater.* **11** 865
[11] Son J H 2009 *J. Appl. Phys.* **105** 102033
[12] Woodward R M, Cole B E, Wallace V P et al 2002 *Phys. Med. Biol.* **47** 3853
[13] Oh S J, Kang J, Maeng I et al 2009 *Opt. Express* **17** 3469
[14] Nagel M, Bolivar P H, Brucherseifer M et al 2002 *Appl. Phys. Lett.* **80** 154
[15] Wu Q, Litz M and Zhang X C 1996 *Appl. Phys. Lett.* **68** 2924
[16] Hu B B, Zhang X C, Auston D H et al 1990 *Appl. Phys. Lett.* **56** 506
[17] Xie X, Dai J and Zhang X C 2006 *Phys. Rev. Lett.* **96** 075005
[18] Chen C Y, Hsieh C F, Lin Y F et al 2004 *Opt. Express* **12** 2625
[19] Rodriguez B S, Yan R, Kelly M M et al 2012 *Nat. Commun.* **3** 780
[20] Ojefors M, Pfeiffer U, Lisauskas A et al 2009 *IEEE J. Solid-State Circuits* **44** 1968
[21] Siegel P H 2002 *IEEE Trans. Microwave Theory Tech.* **50** 910
[22] Hubers H W 2008 *IEEE J. Sel. Top. Quantum Electron.* **14** 378
[23] Ahmad Z, Lisauskas A, Roskos H G et al 2014 *IEEE Int. Electron Devices Meet.* **14** 92
[24] Westlund A, Sangaré P, Ducournau G et al 2013 *Appl. Phys. Lett.* **103** 133504
[25] Generalov A A, Andersson M A, Yang X X et al 2017 *IEEE Trans. Terahertz Sci. Technol.* **7** 614
[26] Vitiello M S, Coquillat D, Viti L et al 2012 *Nano Lett.* **12** 96
[27] Huang Z M, Tong J C, Huang J G et al 2014 *Adv. Mater.* **26** 6594
[28] Huang Z M, Zhou W, Tong J C et al 2016 *Adv. Mater.* **28** 112
[29] Sundaresan R, Mao B Y, Matloubian M, Chen C D and Pollack G P 1989 *IEEE Trans. Electron Devices* **36** 1740
[30] Assaderaghi F, Shahidi G G, Wagner L et al 1997 *IEEE Electron Device Lett.* **18** 241
[31] Jang S L and Lin H H 1999 *Solid-State Electron.* **43** 2147
[32] Mashanovich G Z, Milošević M M, Nedeljkovic M et al 2011 *Opt. Express* **19** 7112
[33] Tang W W, Liu C L, Wang L et al 2017 *Appl. Phys. Lett.* **111** 153502